

# Properties of a Test Bench to Verify Standard Compliance of Proximity Transponders

M. Gebhart, S. Birnstingl, J. Bruckbauer, E. Merlin

NXP Semiconductors Austria GmbH Styria

[michael.gebhart@nxp.com](mailto:michael.gebhart@nxp.com), [stefan.birnstingl@nxp.com](mailto:stefan.birnstingl@nxp.com), [johannes.bruckbauer@nxp.com](mailto:johannes.bruckbauer@nxp.com), [erich.merlin@nxp.com](mailto:erich.merlin@nxp.com)

**Abstract**—Applications for public transport, electronic government or electronic banking based on ISO/IEC 14443, the Standard for 13.56 MHz Proximity Contactless Chip Technology, require a huge number of integrated transponder chips, which up to now already exceeds 3 billion samples out in the field all over the world. It is a specific attribute of the passive RFID technology, that supply power, command reception and information transmission for the transponder chip is connected to one air interface. This requires to vary and test all parameters in combination, to be able to cover the real application case. We present a modular test bench allowing to combine higher layer protocol tests with analogue parameter variation in the contactless antenna arrangement as specified in the ISO/IEC 10373-6 test standard. As the HF Near Field technology cannot be covered just by relaxed UHF test methods but provides different and specific challenges, we focus on the specified antenna arrangement and explain in detail some of the properties and measurement concepts.

## I. OVERVIEW

Specific applications are defined by separate bodies, e.g. the e-Passport is defined by the International Civil Aviation Organization (ICAO) and Contactless Credit Cards are defined by the Europay, MasterCard and Visa (EMVCo) consortium. These documents, however, are always based on the main Product Standard [1], which describes the system properties in physical layer and geometry (part 1), for the analogue parameters at the air interface (part 2), for the command structure on protocol layer (part 3) and for security and extended functions (part 4). The Product Standard references to a Laboratory Standard [2] which allows to verify the product functionality. This standard mainly describes a coaxial antenna arrangement for testing Transponder Card Standard Compliance, and a Card emulation for testing Reader Standard Compliance. Product Standard and Laboratory Standard are defined by working groups of the International Organization for Standardisation [3].

A modular test bench according to the principle shown in fig. 1 can be used to be able to combine tests on the protocol layer, the analogue parameters and the contactless air interface. Such a test bench, consisting of exchangeable modules, allows quick tests as well as investigations in depth. Functional test cases on protocol layer are

- (intended) state transitions,
- regression tests,
- security functions,
- complete and correct card response.

Tested analogue parameters in general are timing, amplitude, noise. More in detail, test cases cover

- resonance frequency, Card loading effect,
- minimum and maximum operating field,
- modulation pulse shape (Reader to Card)
  - o falling edge steepness,
  - o modulation index / residual carrier,
  - o rising edge steepness,
  - o overshoots / ringing effects,
- Card load modulation (using discrete Fourier Transform to measure the sub-carrier as upper and lower sideband to the 13.56 MHz carrier in the frequency domain),
- delay time between command and response,
- start-up time (to power up the Transponder),
- reset time (to shut down the Transponder).

All measurements are performed in dependence of the  $H$ -field strength which is varied in a range of 1.5 – 7.5 ampere per meter (root mean square). In addition, ambient conditions can be varied, this means mainly the temperature, in special cases also movement or additional noise.

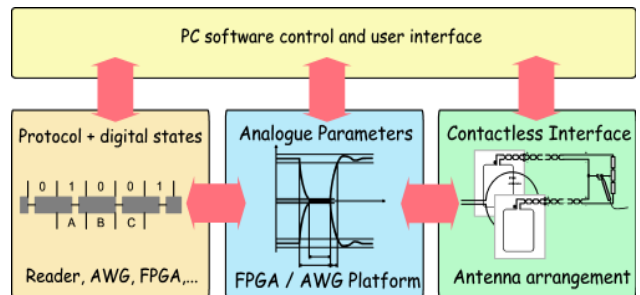


Figure 1. Modular test bench in principle.

All Transponder Card tests are performed on the contactless antenna arrangement as described in the Laboratory Standard. The choice of instruments to connect to the antenna arrangement is not determined in the standard. In the next chapter, we discuss some properties of this antenna arrangement as a background information, which cannot be found in a standard document. This is a necessary pre-condition to understand the complete set-up concept as presented in the last chapter.

## II. CONTACTLESS ANTENNA ARRANGEMENT

The coaxial antenna arrangement as shown in fig. 2 consists of a Proximity Coupling Device (PCD) loop antenna in the center. The Device Under Test (DUT) is placed in 37.5 mm distance on one side to this antenna,

and a Calibration Coil of similar antenna dimensions as a Card is placed on the opposite side to the loop antenna. The PCD antenna in principle emulates properties of a Reader (antenna and matching network). It is used to generate the 13.56 MHz alternating  $H$ -field in the set-up, which is coupled to the Card under test on one side, and to the Calibration Coil used to measure the  $H$ -field strength on the opposite side. In addition, there are two Sense Coils in a Helmholtz arrangement, and their induced voltage is combined in such a way, that the primary field emitted by the PCD antenna is cancelled out and only the secondary  $H$ -field produced by a Transponder Card under Test can be measured.

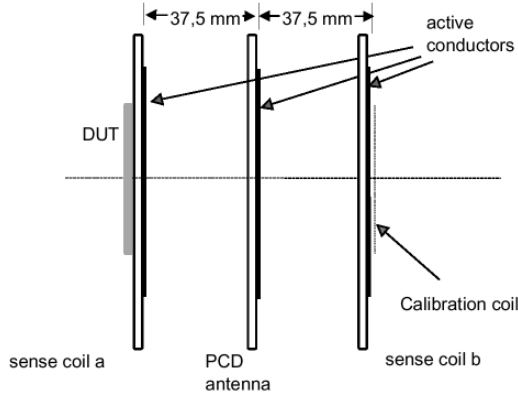


Figure 2. Antenna arrangement according to [2].

The current in the loop antenna is the source for the emitted  $H$ -field, independent whether it is reactive or active current. Like in a real Reader, the reactive current is increased using a higher Q-factor. This allows to emit higher  $H$ -field amplitude on the expense of longer time constants and reduced modulation bandwidth.

#### A. Antenna impedance matching

The inductance of the circular loop antenna can be calculated according to the formula

$$L_{AC} \approx \mu_0 \cdot a \cdot \left[ \ln\left(\frac{8a}{r_w}\right) - 3 \right] \cdot N^2 \quad (1)$$

where  $\mu_0$  is the magnetic field constant  $4\pi \cdot 10^{-7} \text{ Vs/Am}$ ,  $a$  is the PCD antenna radius of 0.075 m,  $r_w$  is the equivalent wire radius of 0.00015 m, according to the specifications in [2]. Only 1 antenna turn  $N$  is connected to the matching network and conducts the current, a second turn with one open end acts as compensation for  $E$ -field emission. This estimation formula gives about 500 Nanohenry loop antenna inductance.

More accurate values can be achieved by a measurement of the printed antenna coil with a Network Analyzer. To minimize measurement errors, the typical way of measuring these parameters consists of two steps: First, the serial inductance and the serial resistance are measured at a frequency well below the self-resonance frequency of the antenna, but high enough for good measurement accuracy. In a second step, the self-resonance frequency of the coil is determined and at this frequency the parallel resistance is measured. Simple calculations then allow to determine the parallel

equivalent circuit of the antenna at the carrier frequency, which is required for the determination of the matching circuit. For a sample PCD antenna coil, at 1 MHz we find  $L_{AM} = 480 \text{ nH}$  and  $R_{DC} = 140 \text{ m}\Omega$ .

The first self-resonance frequency ( $Z$  becomes real) is measured to be 45 MHz. At the self-resonance frequency the parallel resistance is 9.5 k $\Omega$ . The parasitic parallel capacitance of the antenna coil can be calculated from the self-resonance frequency according to

$$\omega_{RES} \cong \frac{1}{\sqrt{L_{AM} C_P}} \Rightarrow \quad (2)$$

$$C_P \cong \frac{1}{(2\pi f_{RES})^2 L_{AM}} \cong 26.06 \text{ pF}$$

The parallel resistance at the self-resonance frequency  $f_{RES}$  is mainly caused by the skin-effect. As the antenna is intended to operate at the carrier frequency  $f_C$  of 13.56 MHz, the value of the resistance has to be corrected according to the frequency dependency of the skin effect, giving a correction factor  $K$  of

$$K = \sqrt{\frac{f_{RES}}{f_C}} \cong 1.82 \quad (3)$$

The parallel resistance at the carrier frequency is

$$R_{P,C} = K \cdot R_{P,RES} \cong 17.3 \text{ k}\Omega \quad (4)$$

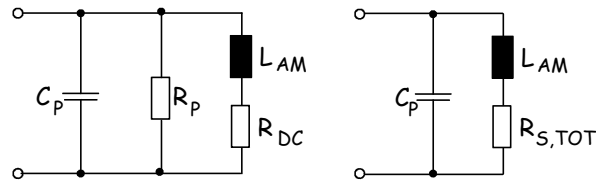


Figure 3. Antenna Equivalent Circuit.

This gives an equivalent circuit of the antenna according to the left side of fig. 3, valid for 13.56 MHz. To achieve an equivalent circuit according to the right side of fig. 3, the parallel resistor has to be re-calculated to a serial resistor for the carrier frequency. We succeed using the general formulas for the Quality factor

$$Q = \frac{\omega L}{R_S} \approx \frac{R_P}{\omega L} \Rightarrow \quad (5)$$

$$R_S = \frac{(\omega_C L_{AM})^2}{R_P} \cong 0.097 \Omega$$

The serial resistors can be added to one resistor

$$R_{S,TOT} = R_{DC} + R_S \cong 237 \text{ m}\Omega \quad (6)$$

As the quality factor  $Q$  is an important parameter in the context, we will also calculate the Q-factor of the antenna coil  $Q_A$ , which is given by

$$Q_A = \frac{\omega_C L_{AM}}{R_{S,TOT}} \cong 172.6 \quad (7)$$

Such a high Q-factor would lead to limited bandwidth and long time constants, causing severe signal distortion in the test setup. So the intended quality factor for the complete antenna circuit is lower, according to the standard at  $Q_C = 35$  to measure at the base data rate of 106 kbit/s. For higher data rates, the PCD antenna may be tuned to lower Q-factors. Adding an external resistor of 0.94 Ohm (5 pieces of 4.7 Ohm resistors in parallel) allows to achieve a Q-factor of about 35.

$$Q_C = \frac{\omega_C L_{AM}}{R_{S,TOT} + R_{EXT}} \cong 34.8 \quad (8)$$

A parallel equivalent resistor has the value

$$R_{P,TOT} = \frac{(\omega_C L_{AM})^2}{R_{S,TOT} + R_{EXT}} \cong 1421 \Omega \quad (9)$$

A parallel equivalent circuit of the PCD loop antenna coil for the RFID carrier frequency of 13.56 MHz according to fig. 3 (right) has the following parameters:

$$L_A \cong 480 \text{ nH}, \quad C_P \cong 26 \text{ pF}, \quad R_{P,TOT} \cong 1.421 \text{ k}\Omega$$

The next important step is to match the load at 13.56 MHz to a 50 Ohm driver impedance  $R_D$ , as used for coaxial connections in laboratories. A simple method is to use a serial capacitor  $C_1$  and a parallel capacitor  $C_2$  as a matching network according to fig. 7. The values of these components can be calculated using the simplified equations (10) and (11). The correct tuning always should be verified with a Network Analyzer.

$$C_1 \approx \frac{1}{\omega_C \sqrt{R_D \cdot R_{P,TOT}}} \cong 44 \text{ pF} \quad (10)$$

$$C_2 \approx \frac{1}{\omega_C^2 \cdot L_A} - C_1 - C_P \cong 217 \text{ pF} \quad (11)$$

In the Laboratory Standard [1], the matching network consists of a fixed value of 47 pF for  $C_1$ , while  $C_2$  is split up into two fixed and one variable capacitor.

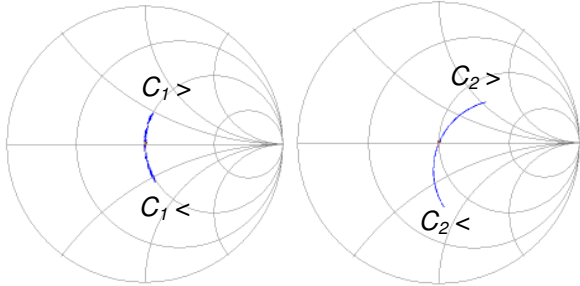


Figure 4. Impedance over frequency, effect of serial capacitor  $C_1$  (left) and parallel capacitor  $C_2$  (right) for tuning in the Smith Chart.

$C_1$  can mainly be used to tune the antenna along a circle of constant real part impedance in the Smith Chart. An increase of the serial capacitor means an increase of the reactive impedance (into the upper, inductive half-plane).  $C_2$  contributes to the reactive and the resistive component, so the adjustable parallel capacitor usually is used to

match the antenna input impedance to a real part close to 50 Ohms.

### B. H-field emitted by PCD antenna

The H-field strength emitted by the loop antenna can be calculated at any target point in the spatial domain using the law of Jean Baptiste Biot and Felix Savart, which is here extended with the retardation potential. It is best to describe the circular PCD antenna in cylindrical (radius  $a$ , angle  $\Phi$ ) parameters at  $z = 0$ .

The radial distance  $r_{SR}$  between a point at the antenna conductor (center position  $x_S, y_S, z_S$ ) and any receive point in space (position  $x_R, y_R, z_R$ ) can be calculated by

$$r_{SR}(\Phi, x_R, y_R, z_R) = \sqrt{(x_S + a \cdot \cos(\Phi) - x_R)^2 + (y_S + a \cdot \sin(\Phi) - y_R)^2 + (z_S - z_R)^2} \quad (12)$$

In the coaxial antenna arrangement with the Transponder Card placed as DUT the  $z$ -component of the H-field is important, as it is perpendicular to the Card antenna. This component  $H_z$  can be calculated for any receive point in space from (13)

$$H_z(x_R, y_R, z_R) = \frac{I_A \cdot a}{4 \cdot \pi} \int_0^{2\pi} \left\{ \frac{e^{-i\beta r_{SR}}}{r_{SR}} \cdot \left( i \cdot \beta + \frac{1}{r_{SR}} \right) \cdot [a + (x_S - x_R) \cdot \cos(\Phi) + (y_S - y_R) \cdot \sin(\Phi)] \right\} d\Phi \quad (13)$$

where  $a$  is the antenna radius,  $\beta$  is the phase constant  $\beta = \frac{2\pi f_C}{c}$  and  $r_{SR}$  depends on  $\phi$  and the target point position ( $x_R, y_R, z_R$ ) and  $I_A$  is the antenna conductor current.

This concept allows to calculate the  $z$ -component of the radiated H-field based upon the knowledge of the Antenna conductor current. For an unloaded PCD antenna producing a symmetric H-field, the distance of the DUT can be calculated as the position, where a homogenous H-field is achieved over an area which corresponds to the specified Card size (ID-1 according to ISO/IEC 7810). For this reason, a distance of 37.5 mm is chosen in the Standard.

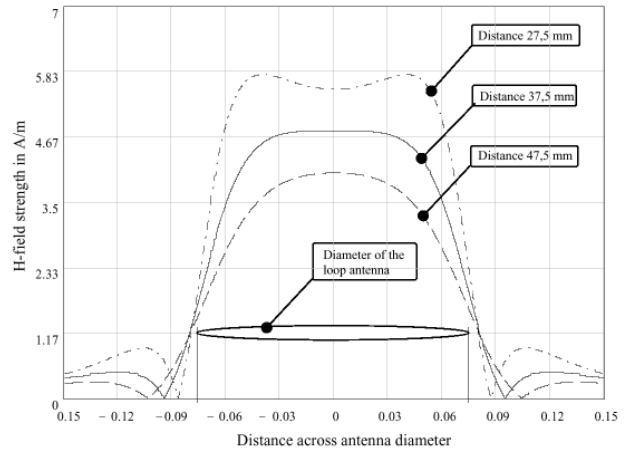


Figure 5.  $H_z$ -field produced by the loop antenna.

The required amplifier driver power can be estimated by (14)

$$P_D \approx \frac{I_A^2 \cdot \omega_C \cdot L_{AM}}{N^2 \cdot Q_C} \quad (14)$$

which results in a minimum of about 0.13 to 3.2 Watts for the specified antenna and  $H$ -field range. To reduce problems caused by load mismatch however, an attenuator should be used, and to allow shorter time constants by the use of antennas with lower  $Q$ -factor, the Lab amplifier should have much more output power, e.g. 75 W, to provide sufficient margin.

Also, the extended Biot-Savart law allows to show the difference for the Near Field and for the Far Field for coaxial and coplanar orientation, as shown for 13.56 MHz in fig. 6.

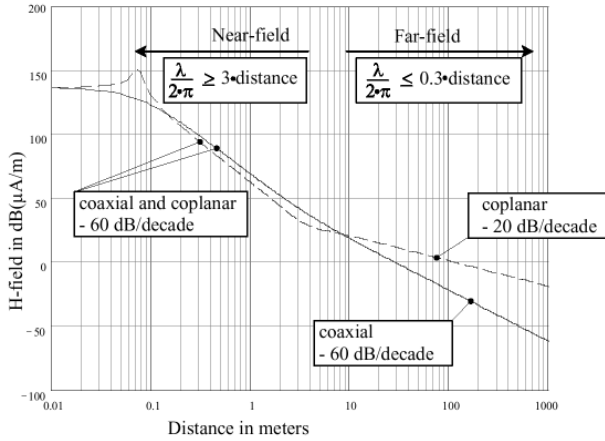


Figure 6.  $H$ -field over distance for coplanar and coaxial orientation.

### C. Modulated $H$ -field in time domain

An option to calculate the time-domain behaviour of the PCD antenna as needed for the modulation pulses is a parametric approach. The falling edge envelope of a 2<sup>nd</sup> order resonant circuit in load matching to the driver output impedance is given by (15)

$$u_F(t) = e^{-t \frac{2f_C \pi}{Q_B}} \quad (15)$$

where  $f_C$  is the carrier frequency and  $Q_B$  is the operational quality factor of the circuit. Accordingly the rising edge envelope is given by (16)

$$u_R(t) = 1 - e^{-t \frac{2f_C \pi}{Q_B}} \quad (16)$$

It is also possible to define a time constant  $\tau$  in this way, that the signal envelope of the falling edge decreases from 1 to  $1/e$ . This means

$$Q_B = \tau \cdot 2 \pi f_C \quad (17)$$

It should be noted, that due to the impedance matching, in practice the operational  $Q$ -factor may slightly differ from the  $Q$ -factor measured for the antenna in the previous section. The so-called *Card Loading Effect* (PCD antenna load mismatch due to the coupling to the Card resonant circuit) and the driver amplifier output stage characteristics also have an influence in practice.

A second option to calculate the time-domain behavior of the PCD antenna network is to use the network function and Laplace transformation. The current in the loop antenna conductor can be calculated from the voltage drop over the external resistor. The Network function  $G(s)$  allows to calculate the voltage across  $R_E$  relative to the voltage at the antenna feed connector using the Laplace-Transformation and the inverse Laplace-Transformation. The network function for the PCD antenna matching network as shown in fig. 7 is given by (18)

$$G(s) = \frac{R_E}{sL_A + R_E + R_{DC}} \cdot \frac{sL_A + R_E + R_{DC}}{s^2 L_A C_2 + sC_2(R_{DC} + R_E) + 1} \cdot \frac{1}{sC_1 + \frac{sL_A + R_E + R_{DC}}{s^2 L_A C_2 + sC_2(R_{DC} + R_E) + 1} + R_D} \quad (18)$$

The antenna current over time  $i_A(t)$  depends on the input voltage  $u_I(t)$  according to (19). As the (active and reactive) current is directly related to the  $H$ -field, this principle allows to calculate the time-domain characteristics of the  $H$ -field emitted by the PCD antenna.

$$i_A(t) = \frac{u_I(t)}{R_E} = \frac{1}{R_E} \cdot L^{-1}\{G(s) \cdot L\{u_I(t)\}\} \quad (19)$$

The challenge in this approach is to consider right all components, including the parasitics.

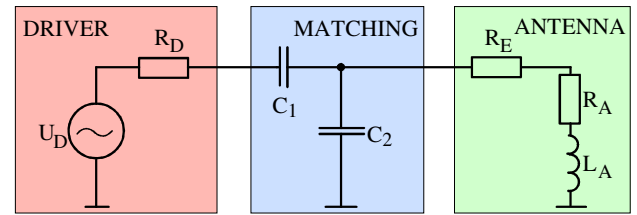


Figure 7. PCD antenna equivalent circuit and matching network.

### D. Measurement of the alternating $H$ -field strength

The alternating  $H$ -field can be measured in space using an open loop coil. A simple but convenient method for a first attempt is to use a scope probe and to connect the tip with the short ground cable. A typical scope input impedance of 1 M $\Omega$  parallel to 12 pF allows to consider this nearly as an open loop. For the Calibration Coil, the antenna outline is specified to 72 x 42 mm, giving an area  $A$  of about 3000 mm<sup>2</sup>. The  $H$ -field (rms) can be derived from the induced voltage (pp), according to (20)

$$H_{RMS} = U_{PP} \cdot \frac{1}{2\pi f_C \cdot \mu_R \mu_0 \cdot A \cdot 2C} = U_{PP} \cdot K \cong U_{PP} \cdot 1.0625 \quad (20)$$

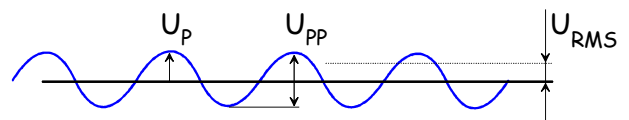


Figure 8. Relations between amplitude values.

In (20),  $U_{pp}$  is the induced open loop voltage (peak-to-peak),  $f_c$  is the carrier frequency of 13.56 MHz,  $\mu$  is the magnetic field constant, and  $C$  is the crest-factor (relating *root mean square* to *peak* values), which for sinusoid wave shapes is  $\sqrt{2}$ .

This relation allows to measure the alternating  $H$ -field perpendicular to the plane of the Calibration Coil and averaged over the coil area, as it is the case in the ISO defined setup.

### III. COMPLETE TEST BENCH

Following the main signal path, the principal function of the test bench as shown in fig. 9 is as follows: A laboratory Reader provides the command sequences as digital modulation signal at logic levels (without carrier). This signal is used to trigger the Analog Signal Generation Block. This component, based on an FPGA, contains sample points for amplitude over time in different memory sections. In the typical operation case, the 13.56 MHz sine wave carrier is produced by the continuous repetition of a small number of sample points out of the memory, which are fed into a D/A converter followed by a low-pass filter and buffer amplifier. Controlled by the digital trigger signal, the Analog Block switches to a different memory section, where a specific pulse shape, modulated on several periods of the sine wave carrier, is stored. At the end of each modulation pulse sequence, the

Analog Block switches back to the memory section for the carrier. In this way, each command can be applied with each pulse shape to the DUT. The modulated signal is then fed into a power amplifier, which allows to control the output amplitude. Over an attenuator (to reduce load mismatch due to the Card detuning and loading effect on the PCD antenna), the modulated carrier is fed into the PCD antenna, which emits the  $H$ -field in the antenna arrangement. The field strength of the carrier is monitored by measurement of the induced voltage of the Calibration Coil by a scope. The Transponder Card under Test will receive the command and respond via Load Modulation. The (secondary) field of the Card is picked up by the Helmholtz arrangement of two symmetrical Sense Coils. This signal is de-coupled by a buffer amplifier with high input impedance ( $> 1\text{M}\Omega // < 14\text{ pF}$ ) and over a 50 Ohm coaxial cable it is fed to channel 2 of the scope, and a second amplifier with automatic gain control (AGC) feeds the Card emission signal to the receive path of the Lab Reader, to avoid overload at higher carrier amplitude or an increased error rate at low amplitude.

In this way it is possible to combine higher layer protocol tests with any pulse shape or modulation index variation, overshoots or ringing effects. All system components can be controlled via PC either by an automated test system or by manual "debug" operation.

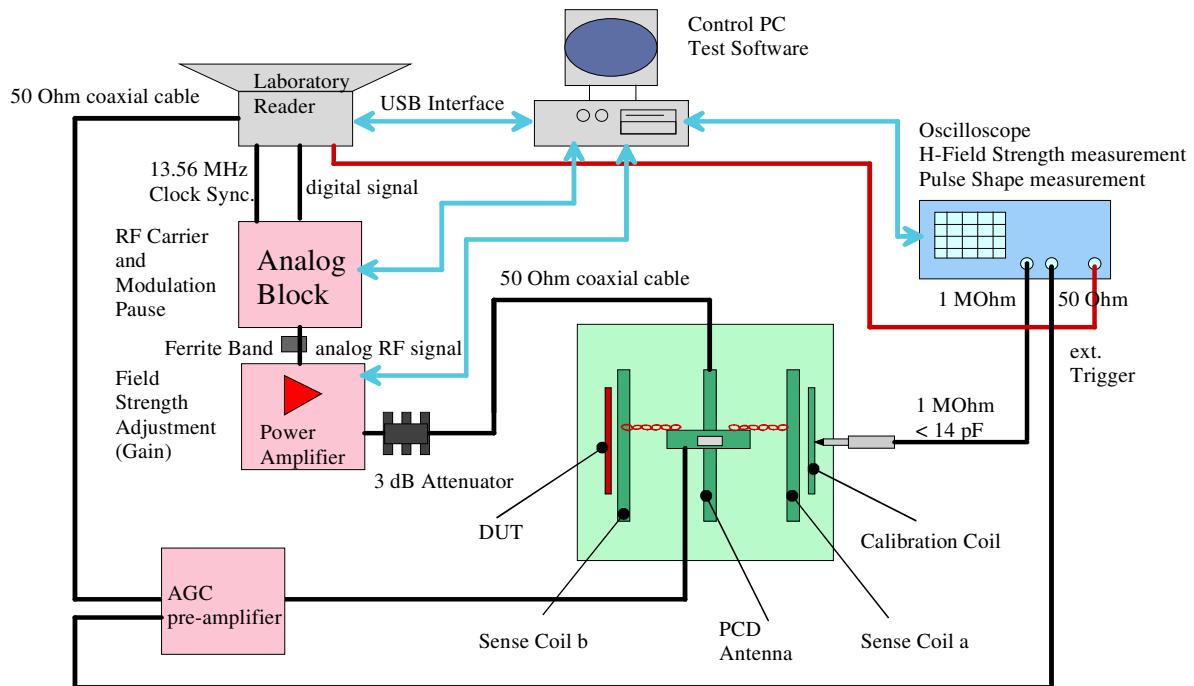


Figure 9. Complete test bench in detail.

### REFERENCES

- [1] ISO/IEC 14443-1/-2/-3/-4: 2001
- [2] ISO/IEC 10373-6: 2000
- [3] ISO/IEC JTC1/SC17/WG8 Homepage ([www.wg8.de](http://www.wg8.de))
- [4] T. Meier et al., Script to RFID session of Lab course "Nachrichtentechnik 2", Dept. of Communication Networks and Satellite Communications, Graz Univ. Tech. 2006
- [5] K. Finkenzeller, RFID-Handbook, Wiley & Sons LTD, ISBN 0-470-84402-7, 2nd edition, 2003, (<http://rfid-handbook.de>)
- [6] D. Paret, RFID and Contactless Smart Card Applications, Wiley-VCH, ISBN 0-470-01195-5, 1st edition 2005